DUAL BAND DUAL PORT COMPACT MIMO ANTENNA FOR MILLIMETER WAVE COMMUNICATION

Project Reference No.: *49S_BE_2273*

College : Cambridge Institute of Technology, K.R. Puram, Bengaluru
Branch : Department of Electronics and communication Engineering
Guide(s) : Dr. Vivek Singh
Student(s) : Ms. Bhoomika
Ms. Bhumika
Ms. Manasa J
Mr. B U SuhaS

Keywords:

2-Port MIMO Antenna, Orthogonal orientation, Radiation Patterns, ECC, DG.

Introduction:

The Wireless communication is evolving fast, needing higher data speeds, better channel capacity, and more efficient use of spectrum. Multiple-Input Multiple-Output (MIMO) technology is key here. MIMO uses multiple antennas at both ends to boost reliability, reduce signal issues, and improve performance without needing more power. For 5G, compact and efficient MIMO antennas are a must for devices and base stations. 5G using millimeter-wave (mm-Wave) frequencies for super-fast data and low latency, the band (24 - 40 GHz) is getting a lot of attention. The mm-waves have challenges like higher signal loss and sensitivity to obstacles, so compact antenna with high gain and low interference are needed for good 5G performance.

In this work a novel dual band dual port MIMO antenna has been investigated and presented. The antenna operates in two frequency bands: 27.7–29.9 GHz and 32.5–35.2 GHz, making it well-suited for high-speed 5G communication. The 2-port MIMO configuration is achieved by placing two elements orthogonally, and additional slots on the ground plane help improve isolation between the ports. The antenna demonstrates good return loss, high gain, and excellent radiation efficiency, while the MIMO system achieves very low ECC and high diversity gain. Overall, the design offers high isolation and efficient performance, making it a strong candidate for next-generation 5G mm-Wave systems.

Objectives:

1. The Design and Simulation: The project entails the design and modelling of a compact dual-band, dual port MIMO antenna structure utilising an RT/ Duroid 5880 substrate.
2. Parametric Analysis: An extensive parametric analysis will be conducted to enhance critical geometric factors affecting bandwidth, matching, and isolation.
3. Performance Evaluation: The antenna's electrical performance will be assessed through simulated S parameters, gain, radiation patterns, efficiency, envelope correlation coefficient (ECC), and directivity gain (DG).
4. Comparative Study: A comparative analysis will cautiously assess the influence of diverse MIMO element orientations and the integration of ground plane slots on isolation and mutual coupling. The research primarily targets the requirements of 5G mm-Wave communications, with potential applicability to other high-frequency wireless systems.
5. Fabrication and testing of the proposed Prototype to validate the simulated findings and industry ready module.

Methodology:

The design of the Dual Band Dual Port Compact MIMO Antenna for millimeter wave communication begins with identifying the target frequency bands, typically in the mmWave range such as 28 GHz and 38 GHz, which are commonly used in 5G applications. The goal is to develop a compact antenna structure that supports dual-band operation and provides two ports for MIMO functionality. A suitable substrate material, such as Rogers RT/Duroid, is selected to ensure low loss and stable performance at high frequencies. Using electromagnetic simulation tools like HFSS or CST, the antenna is designed with careful attention to size, shape, and the placement of the two ports to minimize mutual coupling and ensure good isolation. The design is then optimized through simulations to achieve key performance parameters such as return loss, bandwidth, gain, and radiation pattern. MIMO-specific characteristics such as low envelope correlation coefficient (ECC) and high diversity gain are also analyzed to confirm the antenna's suitability for multiple input multiple output systems. If applicable, the antenna is fabricated and tested using instruments like a Vector Network Analyzer (VNA) to validate the simulated results. The final step involves comparing the measured and simulated data and confirming that the antenna design meets the requirements for compact size, dual-band operation, and effective MIMO performance in millimeter wave communication systems.

Antenna Design and Geometrical Specifications

Single Antenna

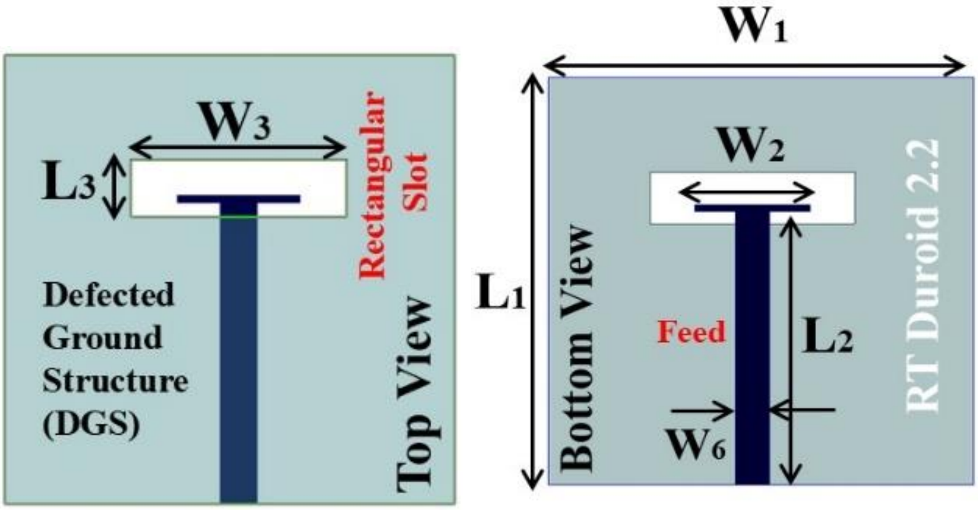

(a) (b)

Figure 1. The Geometrical layout of the single antenna element and (a) Top View, (b) Bottom View of the proposed MIMO antenna.

Proposed single antenna is fabricated over a low loss dielectric substrate, i.e., RT duroid 5880, whose relative permittivity is about $\varepsilon_r \approx 2.2$ and thickness is h = 0.8 mm, which is chosen for effective functioning for mm-wave frequency range as shown in figure 1. The single antenna element of the proposed MIMO design consist a T shape feed line and rectangular slit loaded rectangular ground plane. The design has been optimized through parametric analysis in order to achieve fundamental resonance supporting antenna ranges from 27.70 – 29.90 GHz (2.2 GHz) and 32.50 – 35.20 (2.7 GHz. The 50 Ω microstrip feed line, whose width is designated as W_6, is used to actuate the radiator, providing for sufficient impedance matching. Moreover, geometry of radiator is optimized further in order to enhance resonance as well as broaden operating bandwidth. Geometrical specifications of designed proposed monopole antenna element as well as designed MIMO antenna elements shown are tabulated in Table 1. The entire footprint of antenna is kept in compact form, which makes it suitable for integration in high-density 5G front-end modules.

Table 1. The geometrical specification of the Single Antenna element.

Parameters	Dimensions (mm)
L_1	6.25
L_2	4.2
L_3	0.8
W_1	6.25
W_2	1.7
W_3	3
W_6	0.5

Parametric Investigation

A parametric analysis has been conducted to investigate the effect of length (W_3) and width (L_3) of a rectangular slot and position of radiator (K) to obtain the optimized return loss and maximum bandwidth.

A. Variation in W3 (width of rectangular slot)

The rectangular slot height (W_3) directly controls the effective current path and impedance of the radiator as shown in figure 2(a). At the optimized value (W_3 = 3 mm), the current distribution aligns well with the feed giving maximum resonance and broad bandwidth. If W_3 is too small (2-2.5 mm), the slot is insufficient and the return loss is not very deep around. If W_3 is too large (3.5-4 mm) it disturbs the field distribution and reduces matching. The dip becomes shallow again and resonance shifts slightly. By varying the slot height (W_3), it is observed that the impedance matching and bandwidth are highly sensitive to the parameters. The proposed dimension (W_3) is 3 mm achieves best results.

B. Variation in L_3 (length of the rectangular slot)

The $|S_{11}|$ plots with different values of L_3 is shown in figure 2(b). From the perusal of figure 2(b) it is clear that the variation of L_3 is affecting the lower resonating frequency significantly as compared to the higher resonating frequency. The rectangular slot width (L_3) is directly influences the effective current path of the antenna. As the value of L_3 increases, the return loss at lower resonating frequency also increases making it obsolete while at higher resonating frequency slightly shift towards the higher frequency range has been observed. As the value of L_3 is increasing the dual band is converted into single wide band. At the optimized value that is (L_3 = 0.8 mm), the slot couples efficiently with the radiator. From the parametric study of L_3 variation it is observed that the length of rectangular slot has a significant effect on bandwidth. For smaller values of L_3 (0.4 mm, 0.6 mm), the antenna exhibits poor return loss and reduced bandwidth. However, further increase (1.0 mm, 1.2

mm), leads to degradation in return loss and slight frequency shift, confirming that 0.8 mm is optimum for the band.

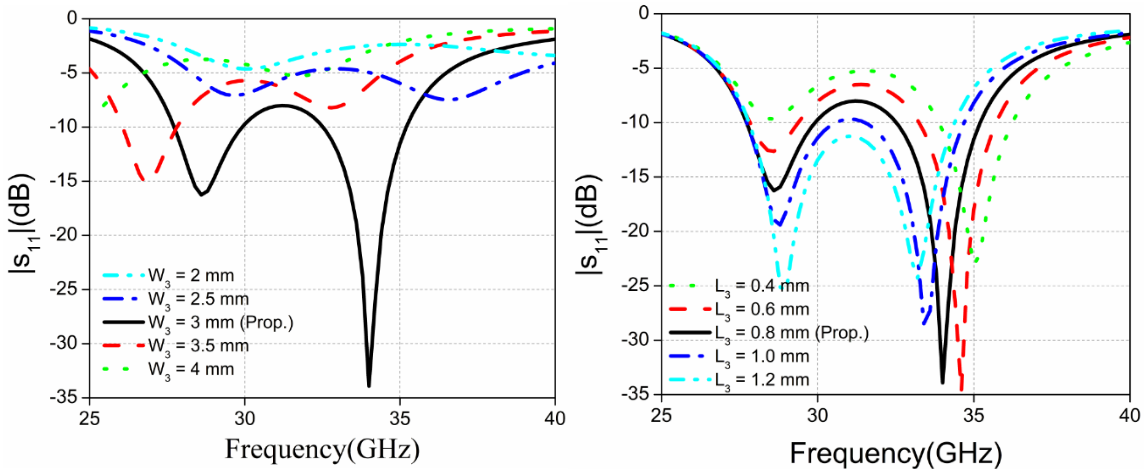

(a) (b)

Figure 2 The parametric investigation by varying the (a) W_3 variation ,(b) L_3 variation.

C. Variation in W_2 (Length of the feed)

Figure 3(a) shows the effect of varying W_2 from 1.5-1.9 mm. As W_2 increases the lower resonance frequency shifts slightly towards lower frequency while higher resonating frequency is not get affected. W_2 = 1.7 mm is marked as the proposed value showing good matching in both bands. If we increase W_2 beyond the optimal value, the feed line becomes stronger in its transformation effect- its impedance and length shift such that the matching to the antenna worsens, the resonance dip moves and the depth of $|S_{11}|$ dip becomes shallower. In that case if we decrease W_2 below the optimal, the feed becomes weaker in matching, again creating impedance mismatch.

D. Variation in K (width of the feed)

The figure 3(b) shows the effect of varying K (0.1mm to 0.5mm) on return loss characteristics. As we increase K there is a major shift is observed in the lower resonance frequencies with continuously increment in return loss. While at higher resonating frequency the effect of increasing the K is minor. The matching in the lower band seems to get affected with increase in K. At K=0.1 mm the proposed value, showing good matching characters. When K is increased, the coupling between feed and patch is weakened, so the resonant dips move and matching degrades.

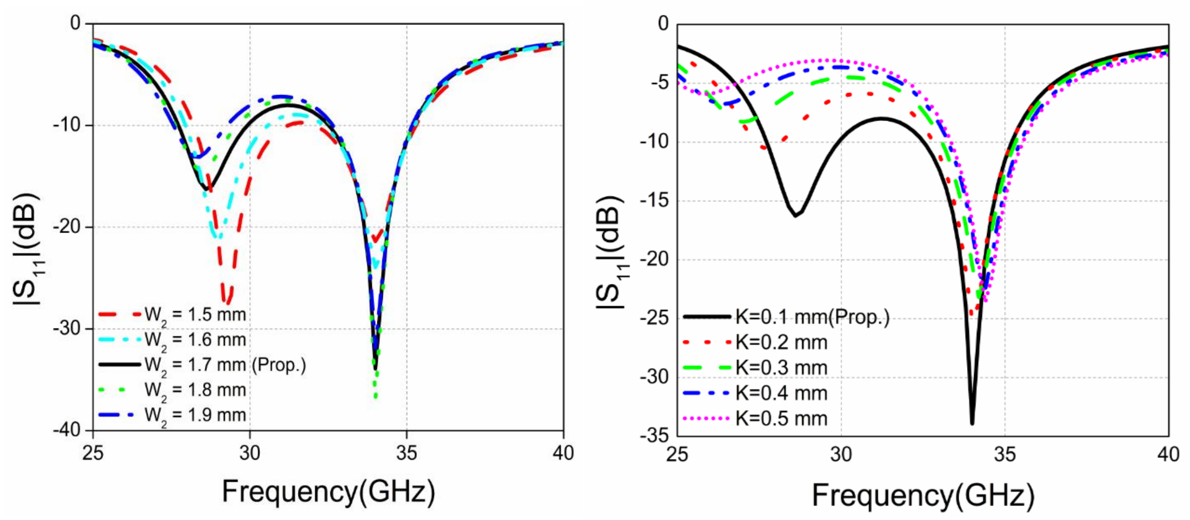

(a) (b)

Figure 3 The parametric investigation by varying the (a) W_2 variation ,(b) K variation.

MIMO Antenna

Figures 4 and figure 5 provide a comparative analysis of several MIMO antennas by replicating the same antenna element in different orientations and assessing their return loss and isolation, respectively. Figure 4 examines four distinct MIMO antenna orientations: side by side of the antenna components, front-to-front positioning, orthogonal arrangement of the antenna units, and anti-parallel antenna placement. Upon examining figure 5ab), it is evident that for all the orientation the variations of $|S_{11}|$ and $|S_{22}|$ are approximately same and return loss is upto -20 dB.

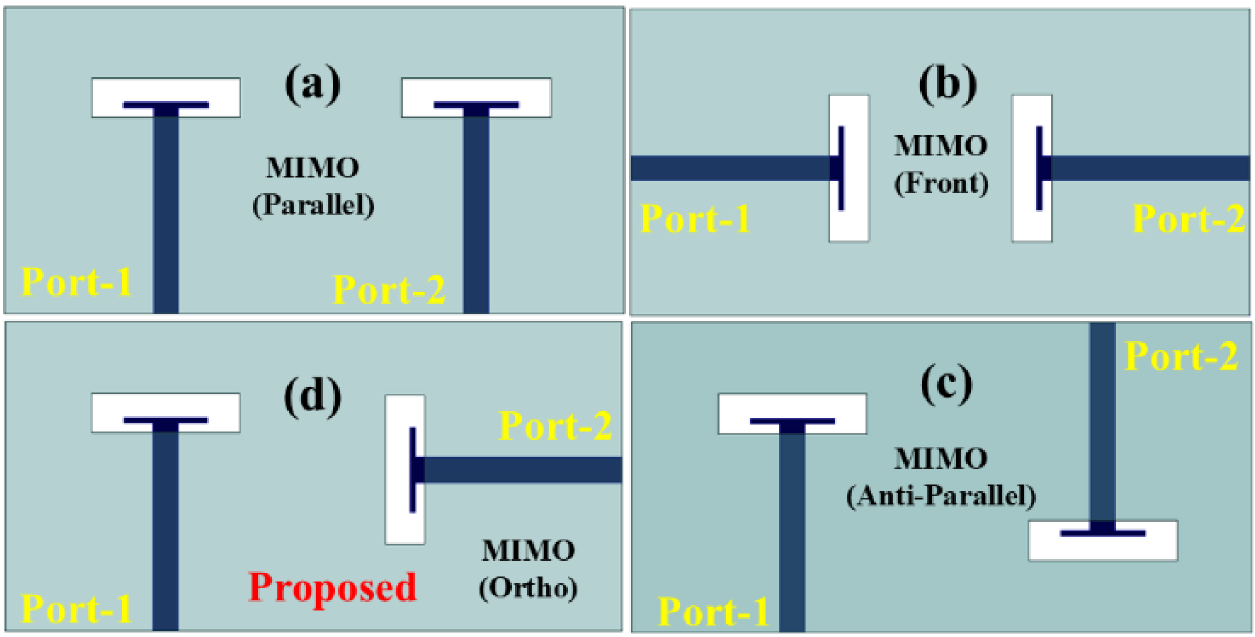

Figure 4. The different orientation of MIMO antenna (a) Parallel, (b) Front to Front, (c) Anti-Parallel, (d) Orthogonal (proposed).

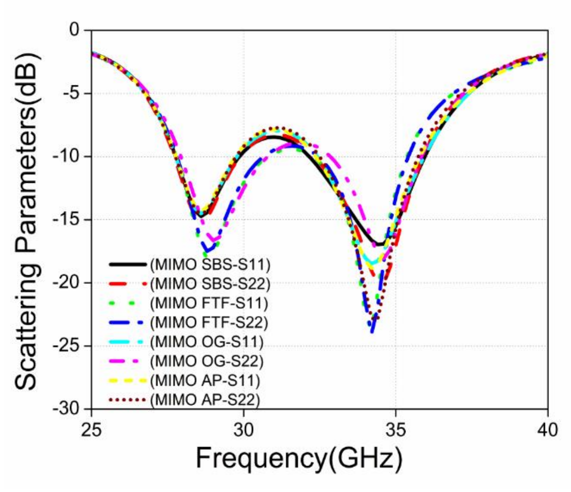

(a)

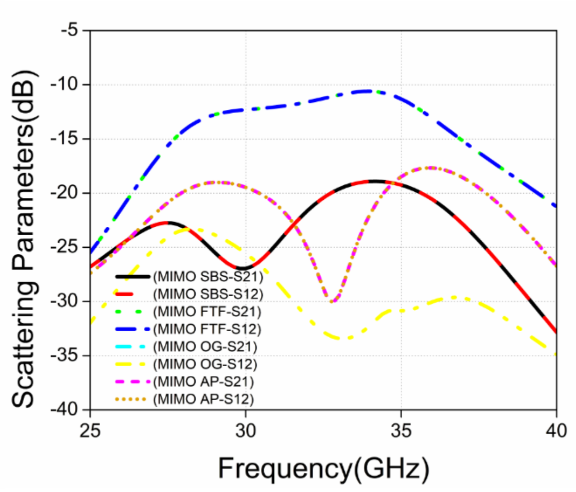

(b)

Figure 5. (a) MIMO Orientation (b) $|S_{11}|$, $|S_{22}|$ plots for different MIMO orientations.

The patterns for various MIMO antenna orientations are depicted in Figure 4 shows the four ways to place two antennas in a MIMO system. In figure 4(a), both antennas are placed side by side in the same direction, which is called Parallel, but they can interfere with each other. In figure 4 (b), the antennas face each other, called front to front, which may still cause interference. In figure 4 (c), the antennas are placed in opposite direction, called the Anti-parallel, which helps to reduce some interference. In figure 4 (d), the antennas are placed at a 90 degree angle to each other, one vertical and one horizontal. This is called Ortho(orthogonal) and it is the proposed method because it gives the best performance by reducing interference between the antennas.

Figure 5(a) shows the return losses of both antenna elements in different MIMO orientations. We see multiple curves but overall the resonant dips for $|S_{11}|$ and $|S_{22}|$ occur near the same frequency, which means both elements are similarly matched in those configurations. Differences in depth or slight shifts reflect how different orientations affect each elements' matching. Figure 5(b) shows isolation or coupling between the two antenna ports under those orthogonal orientations are very low that is below -25dB, meaning good isolation, while in other orientations coupling is higher that is less negative. So depending on the orientation of the two radiators, the mutual coupling changes significantly.

MIMO antenna with and without rectangular slot

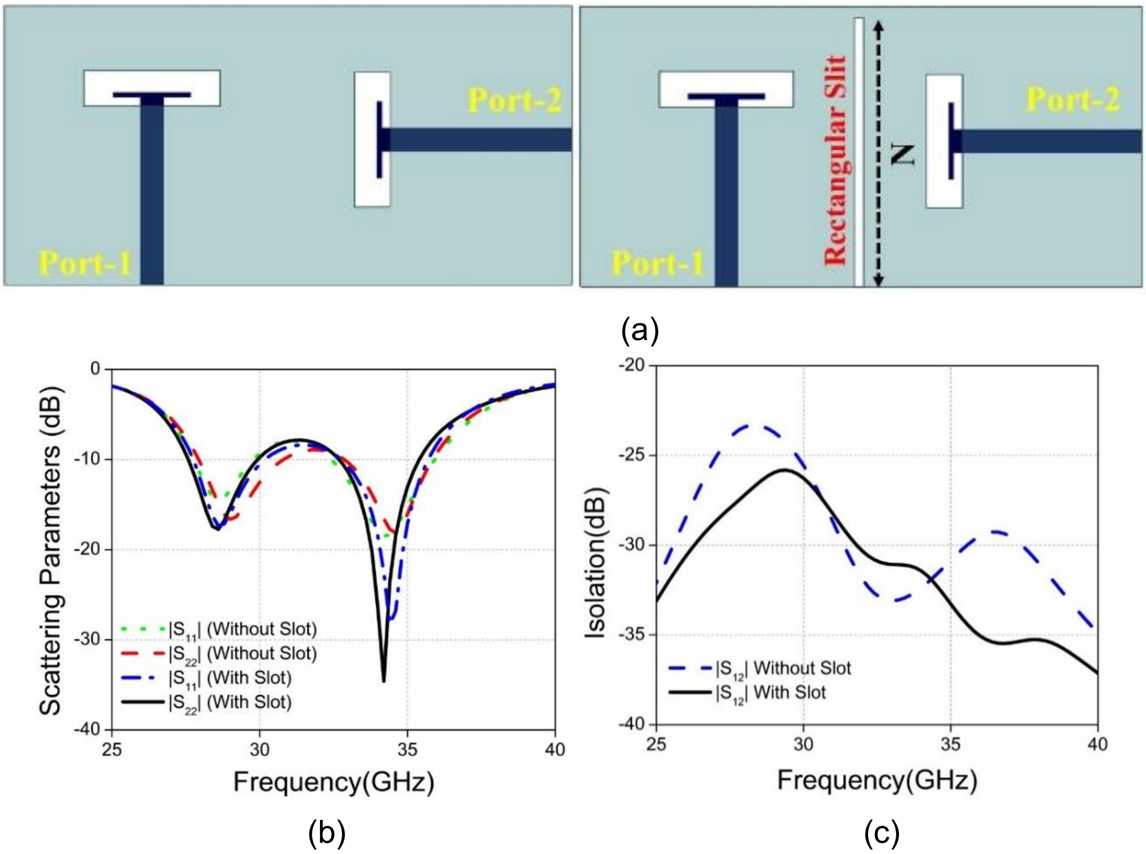

Fig 6 MIMO with and without rectangular slot, (a) Schematic Layout (b) $|S_{11}|$, $|S_{22}|$ plots, (c) Isolation

Figure 6 illustrates the effect of introducing a rectangular slot between the radiating elements of the proposed MIMO antenna. The simulated results are compared for the cases with slot and without slot.

Figure 6(b) shows that both configurations maintain good impedance matching across the operating band. However the antenna with the rectangular slot exhibits deeper notches, indicating improved return loss and slightly better matching performance. Figure 6(c) shows the isolation characteristics between antenna ports. Without the slot, the isolation remains limited around -23 dB for lower band and 30 dB for higher band. By introducing the slot, the isolation improves significantly by 5 dB across the band, which reduces mutual coupling between elements. Thus the rectangular slot effectively enhances the isolation between the ports while maintaining good impedance matching, making the antenna more suitable for MIMO application in mm Wave band.

Surface Current Distribution

Figure 7 shows the electric field distribution for the proposed MIMO antenna, both with and without the rectangular slot. The current is strongest near the feed of the radiating structure, which means that these parts are mostly what makes the structure resonate in the desired frequency band. There is also a strong electric field in the feed line of each antenna element. The anti-parallel positioning of the antenna elements also makes the coupling fields between the antenna parts weaker. Figure 7 shows that the electric field coupling between the ports is stronger than the coupling between the ports when rectangular slots are added. The rectangular slot acts like a neutralisation line (NL), which stops the surface current from moving from one port to another, which improves the isolation. Figure 7(a) shows the strength of the E-Filed when there was no NL, and figure 7(b) shows the strength of the E-Filed when NL was added.

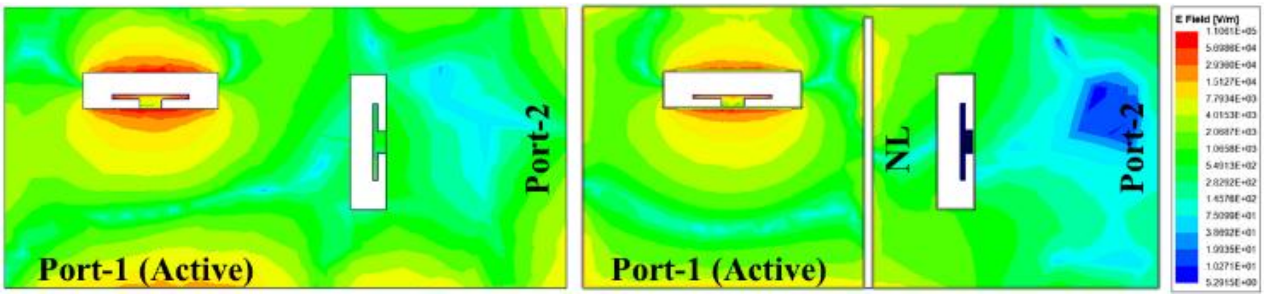

(a) (b)

Figure 7 Surface current distributions (a) Without NL, (b) Without NL.

Result and Conclusion:

An analysis and presentation of the results of the proposed antenna are included in this section. A representation of the impedance bandwidth of the antenna element is provided by the S-parameters that are shown in Figure 8. According to the findings of the study of Figure 8, the impedance bandwidth of the proposed antenna is -10 dB and spans from 27.70 – 29.90 GHz (2.2 GHz) and 32.50 – 35.20 (2.7 GHz).

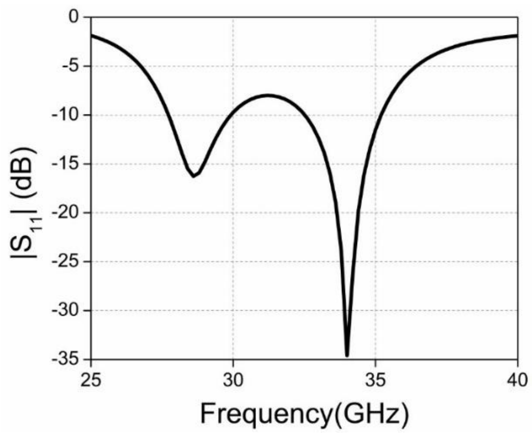

Figure 8. $|S_{11}|$ plots for the proposed antenna.

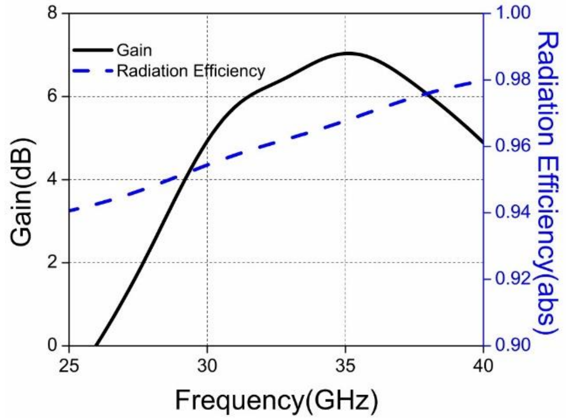

Figure 9. Gain and Radiation efficiency plots for the proposed MIMO antenna.

Figure 9 shows the simulated gain and radiation efficiency of the proposed MIMO antenna. The findings reveal that the gain for lower resonating is approximately 4 dB and around 7 dB for higher resonating frequency. The radiation efficiency graph also reveals that the system works well in resonating areas, with a value of over 94%.

Figure 10 illustrates the two-dimensional radiation patterns (Co and Cross-polarization) that are present in the XoZ-plane for the proposed antenna at both ports for both the frequencies of 28 GHz and 34 GHz. In broadside orientations, the co-polarization levels in both planes are higher than the cross-polarization values by a margin of 15-20 decibel differences. Based on the analysis of radiation patterns, it has been shown that the orthogonal arrangement of antenna elements has been responsible for the achievement of pattern variety.

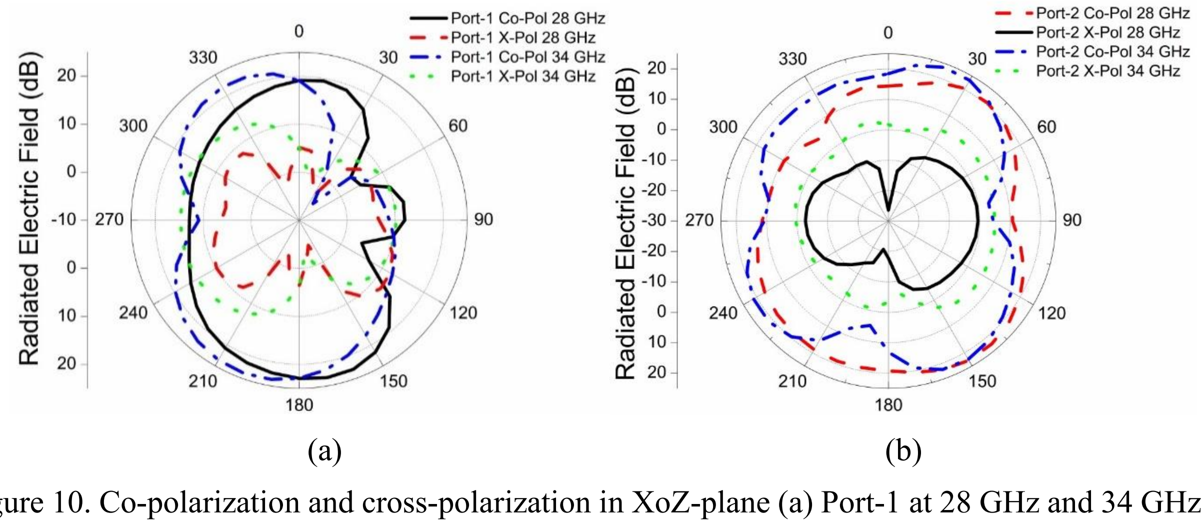

(a) (b)

Figure 10. Co-polarization and cross-polarization in XoZ-plane (a) Port-1 at 28 GHz and 34 GHz (b) Port-2 at 28 GHz and 34 GHz.

MIMO Diversity Performance Matrices

We used the envelope correlation coefficient (ECC) and the diversity gain (DG) to check how well the recommended 2-port MIMO antenna worked for diversity. Figure 11 shows the results of this verification. The effective correlation coefficient (ECC) is the most important measure for figuring out how much correlation there is between antenna ports. Lower values mean that diversity performance is better. The antenna being looked at has ECC values that are much lower than the acceptable limit of 0.5 in the two frequency bands being looked at for operation: 27.70–29.90 GHz (2.2 GHz) and 32.50–35.20 GHz (2.7 GHz). It stays below 0.001 all the time. This result confirms that there is a lot of separation and very little correlation between ports, which makes it a great choice for MIMO applications. During this time, the calculated diversity gain stays very close to the ideal value of 10 dB for the whole range of frequencies, which shows once again how well the antenna works for diversity. The formulas for finding the ECC and DG based on the scattering parameters are equations (1) and (2). [6] These findings indicate that the recommended orthogonal strategy ensures not only superior impedance and gain characteristics but also excellent diversity performance, which is essential for reliable 5G mm-Wave communications.

$$ECC_s = \left| \frac{\left|S_{11}^* S_{12} + S_{21}^* S_{22}\right|}{\left|\left(1-\left|S_{11}\right|^2 - \left|S_{21}\right|^2\right)\left(1-\left|S_{22}\right|^2 - \left|S_{12}\right|^2\right)\right|^{1/2}} \right|^2 \quad (1)$$

$$\mathrm{DG} = 10\sqrt{1 - \mathrm{ECC}^2} \quad (2)$$

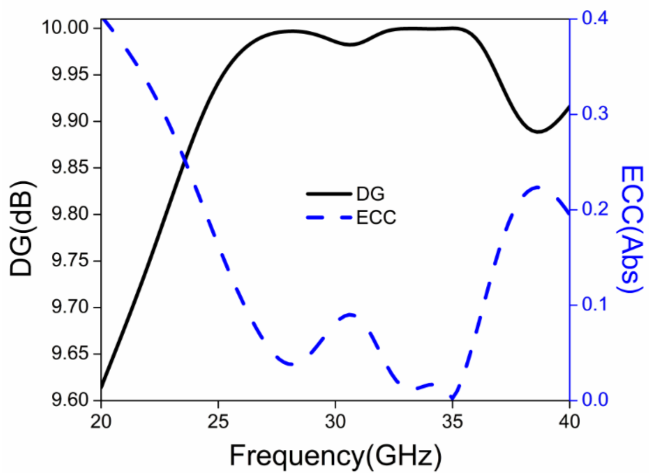

Figure 11. ECC and DG plots for the proposed 2-port MIMO antenna.

References:

1. [1] W. A. Awan *et al.*, “Compact and directional dual band antenna with low mutual coupling MIMO configuration for mm-wave communication,” *Results in Engineering*, vol. 26, p. 105457, Jun. 2025, doi: 10.1016/j.rineng.2025.105457.
2. [2] M. Mahaboob Basha, P. Pradeep, S. Gundala, and J. Syed, “Design of compact and high gain dual-band four-port MIMO antenna array for mm-wave 5G Communications,” *Results in Engineering*, vol. 25, p. 104153, Mar. 2025, doi: 10.1016/j.rineng.2025.104153.
3. [3] W. T. Sethi, S. H. Kiani, M. E. Munir, D. A. Sehrai, H. şerif savci, and D. Awan, “Pattern Diversity Based Four-Element Dual-band MIMO Patch Antenna for 5G mmWave Communication Networks,” *J Infrared Millim Terahertz Waves*, vol. 45, no. 5–6, pp. 521–537, Jun. 2024, doi: 10.1007/s10762-024-00983-0.
4. [4] C. R. Jetti *et al.*, “Design and Analysis of Modified U-Shaped Four Element MIMO Antenna for Dual-Band 5G Millimeter Wave Applications,” *Micromachines (Basel)*, vol. 14, no. 8, p. 1545, Jul. 2023, doi: 10.3390/mi14081545.
5. [5] P. Tiwari *et al.*, “A high isolated, high gain millimeter wave quad-port MIMO antenna array for wideband 5G new radio application,” *Sci Rep*, vol. 15, no. 1, p. 34484, Oct. 2025, doi: 10.1038/s41598-025-18805-1.
6. [6] A. K. Singh, A. K. Dwivedi, C. Choubey, and V. Singh, “Design and Investigation of Compact Backed Mirror Two-Port MIMO Antenna for n257 (30 GHz) 5G Spectrum,” *J Infrared Millim Terahertz Waves*, vol. 45, no. 5–6, pp. 538–555, Jun. 2024, doi: 10.1007/s10762-024-00982-1.

Future Scope:

1. **Extension to Higher Frequency Bands (6G and THz Applications)**
   The antenna design can be further extended to operate in higher frequency ranges such as sub-THz and THz bands, which are expected to be key enablers for future 6G communication systems. This will support ultra-high data rates, holographic communication, and advanced sensing applications.
2. **Miniaturization and System-on-Chip (SoC) Integration**
   Further reduction in antenna size can be explored to enable seamless integration into compact wireless devices, IoT modules, and mobile handsets. Integration with RF front-end circuits using System-on-Chip (SoC) or System-in-Package (SiP) technologies is another potential direction.
3. **Application in Emerging Technologies**
   The proposed antenna can be explored for applications in:
   I. Autonomous vehicles (V2X communication)
   II. Smart cities and IoT networks
   III. Satellite and space communication systems
   IV. Biomedical sensing and imaging systems